Measurement of product alignment in beam–gas chemiluminescent reactions

Michael G. Prisant, Charles T. Rettner, and Richard N. Zare

Department of Chemistry, Stanford University, Stanford, California 94305
(Received 30 March 1981; accepted 29 April 1981)

A procedure is developed for determining the product rotational alignment in the center of mass frame from polarization measurements of the chemiluminescent atom–diatom exchange reaction $A + BC \rightarrow AB^* + C$ under beam–gas conditions. The degree of product alignment with respect to the initial relative velocity reaches a maximum when all reagent orbital angular momentum appears as product rotational angular momentum. For beam–gas chemiluminescence, this implies a limiting degree of polarization of the product emission referenced to the beam axis about which the initial relative velocities are cylindrically symmetric. Calculations are carried out to determine this limiting chemiluminescent polarization for a wide range of beam-gas reaction conditions. Averages over initial conditions are performed by Monte Carlo sampling. These calculations show that under realistic conditions the degree of beam–beam polarization does not exceed twice that of beam–gas polarization. Product polarization is measured in the beam–gas chemiluminescent reaction $Ca(^1D) + HCl \rightarrow CaCl(B^2\Sigma^+) + H$ and found to be greater than 20%. Because of kinematic constraints, this value closely approaches the calculated limiting polarization.

I. INTRODUCTION

Our current understanding of chemical reactions is based primarily on determinations of *scalar* quantities, such as rate constants, cross sections, product state distributions, etc. In particular, studies of state-to-state reaction dynamics can reveal the detailed balance sheet of conservation of energy, such as the effectiveness of reagent energy in promoting reactions and the partitioning of the excess energy of reaction among products.[1–3] In contrast, the analysis of *vector* or *directional* properties of chemical reaction is required to understand the balance sheet for conservation of angular momentum. Thus far such studies have emphasized the determination of product angular distributions.[1–3] These measurements relate the direction of the orbital (external) angular momentum of the products $\mathbf{L}'$ to the initial relative velocity of the reagents $\mathbf{k}$. The corresponding relation of the direction of the internal angular momentum $\mathbf{J}'$ of the products to $\mathbf{k}$ has received much less attention, although its importance as a means of characterizing reaction dynamics was recognized by Herschbach[4] early in the development of molecular beam scattering studies. What experimental information that is available has been obtained from the measurement of polarized chemiluminescence,[5–9] the electric field deflection of polar reaction products,[10–13] and laser induced fluorescence of product molecules.[14] In anticipation that improved techniques would make these and related vector correlations more experimentally accessible, a number of theoretical treatments have appeared.[15–21] This paper examines in detail the polarized chemiluminescence method as applied to beam–gas scattering experiments.

Conservation of angular momentum states that

$$\mathbf{J} + \mathbf{L} = \mathbf{J}' + \mathbf{L}' , \tag{1}$$

where $\mathbf{J}$ represents all internal angular momenta, $\mathbf{L}$ all orbital (external) angular momenta, and the primes refer to products. Because the laboratory direction of $\mathbf{L}$ is at right angles to $\mathbf{k}$ while that of $\mathbf{J}$ is uncorrelated to $\mathbf{k}$, i.e., randomly distributed, there is a tendency for the resultant $\mathbf{J}' + \mathbf{L}'$ to be directed perpendicular to $\mathbf{k}$. The maximum product rotational polarization occurs when $|\mathbf{J}| \ll |\mathbf{L}|$ while $|\mathbf{J}'| \gg |\mathbf{L}'|$. The first condition is often met in practice especially for reactions having large cross reactions, i.e., large impact parameters. The second condition obtains in the kinematically constrained reaction $H' + HL \rightarrow H'H + L$ in which H and L are atoms of high and low mass. In such reactions the departing fragments can carry off little orbital angular momentum and the internal angular momentum of the H'H product is aligned, i.e., in the limit $\mathbf{J}'$ lies parallel to $\mathbf{L}$ in a disk about $\mathbf{k}$.

For the prototype atom transfer reaction $A + BC \rightarrow AB + C$, where BC and AB are diatomic (or quasidiatomic) molecules, the rotational polarization of the AB product may be assessed in a number of ways. Herschbach and co-workers[10–13] used inhomogeneous two-pole electric fields to selectively deflect product molecules in different spatial orientations. Although valuable, this approach determines the alignment averaged over all product states. Moreover, this approach has so far been restricted to the study of highly polar alkali halide products. More recently, it has been suggested[16,22,23] that the technique of laser-induced fluorescence (LIF) may provide a sensitive probe of alignment or orientation; in theory, as many as twelve independent vector moments can be obtained using a crossed beam reaction geometry,[16] and individual vibrational–rotational product states can be interrogated. Preliminary results in this laboratory[14] indicate that the successful application of this technique requires a judicious choice of reaction system and laser source. In particular, open-shell diatomic products may become disoriented by the presence of ambient magnetic fields that cause Larmor precession between the time of formation and the time of detection.[14] Moreover, cw laser sources may prove preferable over pulsed laser sources because the former present less severe optical pumping problems.[24,25] A third approach utilized the intrinsic fluorescence produced by reactions

 0021-9606/81/172222-09$01.00

yielding electronically excited products.[5-9] Jonah *et al.*[5] demonstrated that the degree of (linear) polarization of the molecular chemiluminescence (CL) can be related to the alignment of the product molecules in the laboratory frame. Resolution of the CL spectrum can readily provide polarization measurements for individual vibrational bands. Although this method is blind to the vast majority of (dark) reactions, the comparative experimental simplicity of analyzing the degree of polarization of chemiluminescent emission makes it appealing, when applicable. This approach has been utilized recently in crossed supersonic molecular beam studies,[6-9] providing the first information about the energy dependence of angular momentum alignment in reactive collisions.

Although a crossed-beam geometry has been employed in all but one CL polarization study, single-collision CL reactions are most commonly carried out by firing a reagent (metal) beam into a low-pressure target (oxidant) gas.[1,26] This so-called beam–gas geometry provides essentially maximum single-collision signal intensities, and hence maximum product state selection, at the sacrifice of definition of $\mathbf{k}$ for each reactive collision. With this in mind and in light of the renewed interest in CL polarization studies,[6-9] we have reexamined the problems associated with extracting meaningful information about angular momentum disposal from CL polarization measurements using a beam-gas scattering geometry.

At first glance the intrinsically poor definition of initial relative velocity per reactive collision might be thought to prohibit the accurate measurement of vector properties of the reaction. However, further inspection shows that the averaging process may be turned into an advantage. The distribution of relative velocity vectors is so well defined that the averaging process can be quantitatively calculated to high accuracy. Although the averaging over all possible target molecule velocities diminishes the apparent degree of CL polarization, we shall show that in most cases of practical interest the degree of polarization is reduced by less than 50% from that of a crossed-beam geometry. In what follows we fully develop the analysis begun by Jonah *et al.*[5] We illustrate this approach with new CL polarization data for the $H' + HL \rightarrow H'H + L$ reaction

$$Ca(^1D_2) + HCl \rightarrow CaCl(B\,^2\Sigma^+) + H \ .$$

We also apply this analysis to the results of the kinematically unconstrained reaction $Ba + NO_2 \rightarrow BaO^* + NO$ previously studied.[5]

II. THEORY

A. From chemiluminescent polarization to rotational alignment

In the classical limit, the angular momentum J of a diatomic molecule is perpendicular to the internuclear axis. The emission properties may be represented by a Hertzian dipole oscillator μ, which is rigidly attached to the molecular framework. Symmetry rules permit two types of electronic transitions for diatomic molecules. For a parallel-type transition ($\Delta\Lambda = 0$), μ lies along the internuclear axis, while for a perpendicular-type transition ($\Delta\Lambda = \pm 1$), μ is perpendicular to the internuclear axis, either along J for a Q line ($\Delta J = 0$) or in the plane of rotation for R and P lines ($\Delta J = \pm 1$).

An oscillating electric dipole emits light whose electric vector (polarization vector) lies parallel to its axis of oscillation. Because this axis is well defined relative to the molecular framework of a radiating diatomic molecule, the degree of linear polarization of such radiation reflects the molecular alignment, i.e., the alignment of the angular momentum vector J in space. Thus, the polarization of CL can be related to the distribution of angular momentum vectors of the emitting molecule.[5]

For a beam–gas configuration the chemiluminescence is traditionally viewed at right angles to the beam axis. Let $I_\parallel$ and $I_\perp$ denote the CL intensities polarized parallel and perpendicular to the beam axis. Then the degree of polarization P of the chemiluminescence is defined by

$$P = (I_\parallel - I_\perp)/(I_\parallel + I_\perp) \ . \tag{2}$$

Since there is cylindrical symmetry about the beam axis, the product $\mathbf{J}'$ distribution can be expressed as a Legendre expansion

$$f(\hat{\mathbf{J}}' \cdot \hat{\mathbf{Z}}) = \sum_l a_l P_l(\hat{\mathbf{J}}' \cdot \hat{\mathbf{Z}}) \ . \tag{3}$$

Here $\hat{\mathbf{J}}'$ is the unit vector along $\mathbf{J}'$, $\hat{\mathbf{Z}}$ is the unit vector along the beam axis,

$$\hat{\mathbf{J}}' \cdot \hat{\mathbf{Z}} = \cos\theta \tag{4}$$

is the cosine of the angle included by $\hat{\mathbf{J}}'$ and $\hat{\mathbf{Z}}$, and the coefficients

$$a_l = \frac{2l+1}{2} \int_{-1}^{1} P_l(\hat{\mathbf{J}}' \cdot \hat{\mathbf{Z}}) f(\hat{\mathbf{J}}' \cdot \hat{\mathbf{Z}})\, d(\hat{\mathbf{J}}' \cdot \hat{\mathbf{Z}})$$

$$= \frac{2l+1}{2} \langle P_l(\hat{\mathbf{J}}' \cdot \hat{\mathbf{Z}}) \rangle \tag{5}$$

are the lth Legendre moments of the distribution $f(\hat{\mathbf{J}} \cdot \hat{\mathbf{Z}})$. The degree of polarization is then given by[5]

$$P(P, R \text{ line}) = -3\alpha/(20 - \alpha) \tag{6}$$

for both a parallel-type transition in which μ lies along the internuclear axis and for a perpendicular-type transition in which μ lies in the plane of rotation perpendicular to the internuclear axis. Similarly,

$$P(Q \text{ line}) = 3\alpha/(10 + \alpha) \tag{7}$$

for a perpendicular-type transition in which μ lies along $\mathbf{J}'$. Here α is the alignment parameter

$$\alpha = a_2/a_0$$

$$= \frac{\frac{5}{2}\langle P_2(\hat{\mathbf{J}}' \cdot \hat{\mathbf{Z}}) \rangle}{\frac{1}{2}\langle P_0(\hat{\mathbf{J}}' \cdot \hat{\mathbf{Z}}) \rangle}$$

$$= 5\langle P_2(\hat{\mathbf{J}}' \cdot \hat{\mathbf{Z}}) \rangle \tag{8}$$

which is proportional to the second Legendre moment of $f(\hat{\mathbf{J}}' \cdot \hat{\mathbf{Z}})$. In Eq. (8) we have set $\langle P_0(\hat{\mathbf{J}}' \cdot \hat{\mathbf{Z}}) \rangle = 1$. Alternatively, Eqs. (6) and (7) may be expressed in terms of the average cosine square of the angle between $\hat{\mathbf{J}}'$ and $\hat{\mathbf{Z}}$, i.e.,

$$\langle \cos^2\theta \rangle = \langle |\hat{\mathbf{J}}' \cdot \hat{\mathbf{Z}}|^2 \rangle \ . \tag{9}$$

We find

$$P(P, R \text{ line}) = \frac{1 - 3\langle \cos^2\theta \rangle}{3 - \langle \cos^2\theta \rangle} \ , \tag{10}$$

and

$$P(Q \text{ line}) = \frac{3\langle \cos^2\theta \rangle - 1}{1 + \langle \cos^2\theta \rangle} \ . \tag{11}$$

Typically, individual rotational branches are not resolved in electronic CL studies. For a parallel-type transition, there are only P and R lines in the classical limit while for a perpendicular-type transition, Q lines as well as P and R lines are present. The choice of parallel-type transitions considerably simplifies the extraction of molecular alignment from CL polarization. In what follows we confine our discussion to this case and set $P \equiv P(P, R \text{ line})$. These relationships set limits on our ability to examine the laboratory $\hat{\mathbf{J}}'$ distribution of the reaction products via polarization measurements. Dipole emission polarization never reveals the Legendre moments of the emitter orientational distribution beyond second order. Further, the odd moments must vanish as a consequence of the symmetry of the system when the chemiluminescence is viewed at right angles to the beam axis. The emitted light *cannot* be circularly polarized in such a beam–gas configuration.

B. From rotational alignment in the laboratory frame to rotational alignment in the center of mass

The observed degree of polarization P always yields the alignment parameter α for the distribution $f_{\text{obs}}(\hat{\mathbf{J}}' \cdot \hat{\mathbf{Z}})$ of $\mathbf{J}'$ directions about the beam axis. To understand the dynamical origin of α, one must consider how the $f_{\text{obs}}(\hat{\mathbf{J}}' \cdot \hat{\mathbf{Z}})$ distribution is built from the center-of-mass distribution $f_{\text{c.m.}}(\hat{\mathbf{J}}' \cdot \hat{\mathbf{k}})$ of $\mathbf{J}'$ directions about the relative velocity $\mathbf{k}$. The $f_{\text{obs}}(\hat{\mathbf{J}}' \cdot \hat{\mathbf{Z}})$ distribution is the result of averaging the $f_{\text{c.m.}}(\hat{\mathbf{J}}' \cdot \hat{\mathbf{k}})$ distribution over the distribution $f_{\text{lab}}(\hat{\mathbf{k}} \cdot \hat{\mathbf{Z}})$ of relative velocity directions $\hat{\mathbf{k}}$ about the beam axis. The laboratory distribution of relative velocity directions in a beam–gas experiment is itself the result of averaging over the distribution of *magnitudes* of $\mathbf{k}$ weighted by the excitation function for the reaction. The distribution $f_{\text{c.m.}}(\hat{\mathbf{J}}' \cdot \hat{\mathbf{k}})$ is, of course, determined by the dynamics of the reaction. Thus these studies offer a glimpse of this distribution via the "keyhole" of its second Legendre moment, from which one learns how the reaction partitions total angular momentum into internal and orbital (external) angular momenta of the products.

Clearly the distribution whose second moment we "observe," $f_{\text{obs}}(\hat{\mathbf{J}}' \cdot \hat{\mathbf{Z}})$, results from $f_{\text{c.m.}}(\hat{\mathbf{J}}' \cdot \hat{\mathbf{k}})$ averaged over $f_{\text{lab}}(\hat{\mathbf{k}} \cdot \hat{\mathbf{Z}})$, i.e.,

$$f_{\text{obs}}(\mathbf{J}' \cdot \mathbf{Z}) = \int f_{\text{c.m.}}(\hat{\mathbf{J}}' \cdot \hat{\mathbf{k}}) f_{\text{lab}}(\hat{\mathbf{k}} \cdot \hat{\mathbf{Z}})\, d\hat{\mathbf{k}} \ , \tag{12}$$

where $d\hat{\mathbf{k}}$ is the infinitesimal dihedral angle element between the $J'k$ and kZ planes. We consider two special cases of Eq. (12).

As the spread of relative velocities narrows, $f_{\text{lab}}(\hat{\mathbf{k}} \cdot \hat{\mathbf{Z}})$ tends to $\delta[(\hat{\mathbf{k}} \cdot \hat{\mathbf{Z}}) - 1]$, $f_{\text{obs}}(\hat{\mathbf{J}}' \cdot \hat{\mathbf{Z}})$ approaches $f_{\text{c.m.}}(\hat{\mathbf{J}}' \cdot \hat{\mathbf{Z}})$, and no deconvolution is necessary to determine $f_{\text{c.m.}}(\hat{\mathbf{J}}' \cdot \hat{\mathbf{k}})$. This limiting case pertains to a beam–gas scattering experiment in which the velocity of the beam species greatly exceeds that of the gas molecules, or to crossed monoenergetic molecular beams. In the latter, Z is defined along the unique relative velocity vector.

Alternatively, when $\hat{\mathbf{J}}'$ always lies in a plane perpendicular to $\hat{\mathbf{k}}$, then $f_{\text{c.m.}}(\hat{\mathbf{J}}' \cdot \hat{\mathbf{k}}) = \delta[(\hat{\mathbf{J}}' \cdot \hat{\mathbf{k}}) - 0]$ and $f_{\text{obs}}(\hat{\mathbf{J}}' \cdot \hat{\mathbf{Z}})$ reflects only the average over relative velocity directions. Physically, this case is approached in the kinematic limit where all the orbital angular momentum of the reagents appears as internal angular momentum of the products and where the reagents have no rotational or spin angular momenta. We call this the rotationless and spinless kinematic limit (RASKL). We expect the limiting polarization, P_{RASKL}, to describe the maximum CL polarization of the $H' + HL \rightarrow H'H^* + L$ reaction system.

In this limit $P_{\text{RASKL}} = 0$ when $f_{\text{lab}}(\hat{\mathbf{k}} \cdot \hat{\mathbf{Z}})$ is an isotropic distribution and $\langle \cos^2\theta \rangle = \frac{1}{3}$, e.g., beam–gas chemiluminescence when the velocities of the gas molecules greatly exceed those of the beam species, and $P_{\text{RASKL}} = \frac{1}{3}$ when $f_{\text{lab}}(\hat{\mathbf{k}} \cdot \hat{\mathbf{Z}}) = \delta[(\hat{\mathbf{k}} \cdot \hat{\mathbf{Z}}) - 1]$ and $\langle \cos^2\theta \rangle = 0$, e.g., beam–gas chemiluminescence when the velocities of the beam species greatly exceed those of the gas. The upper limit is the maximum degree of polarization that can be observed in any beam–gas experiment in which P is measured with respect to the beam axis or in any beam–beam experiment in which P is measured with respect to the relative velocity vector. Of course the above statement refers to a parallel-type transition in the classical limit.

The distribution of $\hat{\mathbf{k}}$ is cylindrical about $\hat{\mathbf{Z}}$ and the distribution of $\hat{\mathbf{J}}'$ is cylindrical about $\hat{\mathbf{k}}$. So long as these distributions are uncorrelated we can write[27,28]

$$\langle P_2(\hat{\mathbf{J}}' \cdot \hat{\mathbf{Z}}) \rangle = \langle P_2(\hat{\mathbf{J}}' \cdot \hat{\mathbf{k}}) \rangle \langle P_2(\hat{\mathbf{k}} \cdot \hat{\mathbf{Z}}) \rangle \ , \tag{13}$$

where $\langle P_2(\hat{\mathbf{J}}' \cdot \hat{\mathbf{Z}}) \rangle \equiv \alpha/5$ and $\langle P_2(\hat{\mathbf{J}}' \cdot \hat{\mathbf{k}}) \rangle$ and $\langle P_2(\hat{\mathbf{k}} \cdot \hat{\mathbf{Z}}) \rangle$ are the second Legendre moments of $f_{\text{c.m.}}(\hat{\mathbf{J}}' \cdot \hat{\mathbf{k}})$ and $f_{\text{lab}}(\hat{\mathbf{k}} \cdot \hat{\mathbf{Z}})$. Thus experimental determination of the alignment parameter α coupled with calculation of $\langle P_2(\hat{\mathbf{k}} \cdot \hat{\mathbf{Z}}) \rangle$ yields the second Legendre moment of the distribution of $\hat{\mathbf{J}}'$ with respect to $\hat{\mathbf{k}}$ in the center-of-mass frame. The dynamical information in this measurement appears in this quantity.

C. Procedure for calculating $\langle P_2(\hat{\mathbf{k}} \cdot \hat{\mathbf{Z}}) \rangle$

We wish to calculate the laboratory distribution of relative velocity directions and its second Legendre moment. We assume that the reaction cross section is constant over the range of relative velocities contributing to the reaction. This calculation also provides the RASKL polarization limit, P_{RASKL}, which is an upper bound on the classical parallel-type polarization of any beam–gas experiment. In the RASKL limit we have

$$\langle P_2(\hat{\mathbf{J}}' \cdot \hat{\mathbf{k}}) \rangle_{\text{RASKL}} = \left\langle P_2\left(\frac{\pi}{2}\right) \right\rangle = -\tfrac{1}{2} \ , \tag{14}$$

because $\mathbf{J}'$ is constrained to lie in a plane perpendicular

to k. We see from Eqs. (8), (13), and (14) that

$$\alpha_{\mathrm{RASKL}} = -\tfrac{5}{2}\langle P_2(\hat{\mathbf{k}}\cdot\hat{\mathbf{Z}})\rangle \ . \tag{15}$$

It follows from Eq. (6) that

$$P_{\mathrm{RASKL}} = \frac{3\langle P_2(\hat{\mathbf{k}}\cdot\hat{\mathbf{Z}})\rangle}{8+\langle P_2(\hat{\mathbf{k}}\cdot\hat{\mathbf{Z}})\rangle} \ . \tag{16}$$

Hence the determination of $\langle P_2(\hat{\mathbf{k}}\cdot\hat{\mathbf{Z}})\rangle$ is equivalent to a knowledge of P_{RASKL}, and vice versa.

The analytic calculation of $f_{\mathrm{lab}}(\hat{\mathbf{k}}\cdot\hat{\mathbf{Z}})$ involves integration over all quantities which affect $\hat{\mathbf{k}}\cdot\hat{\mathbf{Z}}$ and which are not uniquely specified by the experiment. For a beam–gas configuration these quantities include (1) the distribution of magnitudes and directions of the beam velocities, (2) the distribution of magnitudes and directions of the gas velocities, and (3) the distribution of relative velocities that react. Jonah *et al.*[5] attacked this problem by considering the reaction of a monoenergetic beam with a Maxwellian gas. They further simplified the problem by calculating $f_{\mathrm{RASKL}}(\hat{\mathbf{J}}'\cdot\hat{\mathbf{Z}})$ for a fixed magnitude of the relative velocity, v_{rel}, and the beam velocity, v_b; they obtained

$$\alpha_{\mathrm{JOZ}} = \tfrac{5}{2}\,(3X^{-1}\coth X - 3X^{-2} + 1) \ , \tag{17}$$

where $X = (M_g v_{\mathrm{rel}} v_b/kT_g)$ and M_g and T_g are the mass and temperature of the gas species.

This description is insufficient. First, there is no prescription for picking v_{rel} and therefore a judicious choice of X cannot be made. Second, the *exact* value of α_{RASKL} is required to extract $\langle P_2(\hat{\mathbf{J}}'\cdot\hat{\mathbf{k}})\rangle$ through the use of Eqs. (15) and (16). Without such exact values, the beam–gas averaging still hides the dynamical information of $\langle P_2(\hat{\mathbf{J}}'\cdot\hat{\mathbf{k}})\rangle$ that we seek for the chemical reaction system. Moreover, we are unable to set an upper limit on the beam–gas CL polarization. Equation (17) is only an approximation for α_{RASKL}, since the proper averages over $\mathbf{v}_b$ and $\mathbf{k}$ have not been carried out. This was realized by Jonah *et al.*[5] Unfortunately analytical efforts to calculate an exact expression for α_{RASKL} rapidly become intractable. Moreover, we find (see below) that the results of Jonah *et al.*[5] agree with the comprehensive computations presented here only so long as $v_b \gg \langle v_g\rangle$.

The Monte Carlo method[29,30] offers a natural numerical approach to these calculations. This method can be used to calculate $f_{\mathrm{lab}}(\hat{\mathbf{k}}\cdot\hat{\mathbf{Z}})$ by accummulating events determined by the quantities averaged in the experiment. Of course nature "performs" the multidimensional integral that determines $f_{\mathrm{lab}}(\hat{\mathbf{k}}\cdot\hat{\mathbf{Z}})$ in exactly the same way.

A computer program has been written to carry out this calculation.[31] The program selects velocities for the beam and gas species from Maxwellian distributions. The angle between $\mathbf{v}_b$ and $\mathbf{v}_g$ is sampled from a cosine weighted distribution for the beam–gas scattering. The impact parameter b is chosen from a linearly weighted distribution between 0 and b_{max}. This is used to calculate the magnitude of the reagent orbital angular momentum, $|\mathbf{L}|$, which equals the product internal angular momentum $|\mathbf{J}'|$ in the RASKL limit. Note that the choice of b does not affect any of the *directional* distributions calculated. The program then selects the direction of $\hat{\mathbf{J}}'$ relative to $\hat{\mathbf{k}}$. The relevant distribution will depend on the dynamical model chosen for simulation. Here we are concerned only with the RASKL limit, in which $\hat{\mathbf{J}}'$ is confined to a disk perpendicular to $\hat{\mathbf{k}}$ and all azimuthal angles are equiprobable. Next, the calculated values of $\hat{\mathbf{k}}\cdot\hat{\mathbf{Z}}$, $\hat{\mathbf{J}}'\cdot\hat{\mathbf{Z}}$, and $|\mathbf{L}|$ are sorted into histograms. The final count for the event is then weighted by w, where

$$w = |k| \ . \tag{18}$$

This weighting simply reflects the greater flux of reactive events associated with higher relative velocities (assuming that the cross section is independent of $|k|$). After a preset number of reactive events, the program calculates $\langle P_2(\hat{\mathbf{k}}\cdot\hat{\mathbf{Z}})\rangle$, $\langle P_2(\hat{\mathbf{J}}'\cdot\hat{\mathbf{Z}})\rangle_{\mathrm{RASKL}}$ and $\langle|\mathbf{L}|\rangle$ from their respective histograms. The limiting CL polarization P_{RASKL} is then calculated from Eqs. (6) and (8) using the value of $\langle P_2(\hat{\mathbf{J}}'\cdot\hat{\mathbf{Z}})\rangle_{\mathrm{RASKL}}$.

We recognize that P_{RASKL} and α_{RASKL} can be obtained directly from a knowledge of $f_{\mathrm{lab}}(\hat{\mathbf{k}}\cdot\hat{\mathbf{Z}})$, through Eqs. (15) and (16). However, by calculating these from $f(\hat{\mathbf{J}}'\cdot\hat{\mathbf{Z}})$ we facilitate modifications to calculate P and α for a variety of reaction mechanisms. This is possible because the program averages over the mode of angular momentum partitioning.

The convergence of the Monte Carlo method is independent of the dimensionality of the integration. Typically 5000 events are accumulated, giving polarizations to an approximate accuracy of $5000 \pm (5000)^{1/2}$ or $\sim 1.4\%$.

We note the following reduction of parameters in the calculation. The value of $(\hat{\mathbf{k}}\cdot\hat{\mathbf{Z}})$ depends on the speed ratio v_b/v_g and not on the individual magnitudes of these velocities. The distribution of this ratio, and hence the distribution of $(\hat{\mathbf{J}}'\cdot\hat{\mathbf{Z}}) = \cos\theta$ in the RASKL limit is uniquely determined by the ratio

$$\rho = (T_g M_b)/(T_b M_g) \ . \tag{19}$$

Hence $\langle P_2(\hat{\mathbf{k}}\cdot\hat{\mathbf{Z}})\rangle$, α_{RASKL} and P_{RASKL} can be parameterized by ρ for all effusive beam–gas experiments. We call ρ the universal beam–gas parameter.

D. Results of the Monte Carlo calculation

Table I lists the computed values of $\langle P_2(\hat{\mathbf{k}}\cdot\hat{\mathbf{Z}})\rangle$ and α_{RASKL} obtained after accumulation of 5000 events for values of the universal parameter ρ over the range 0.0 to 2.0 at intervals of 0.1. As before, we have chosen the normalization $\langle P_0(\hat{\mathbf{k}}\cdot\hat{\mathbf{Z}})\rangle = 1$. The data are presented in Fig. 1. As ρ increases, both $\langle P_2(\hat{\mathbf{k}}\cdot\hat{\mathbf{Z}})\rangle$ and α_{RASKL} asymptotically approach zero. However, values of ρ greater than unity are rarely encountered in practice. Of course, ρ refers strictly to an effusive beam; for a nozzle beam Fig. 1 must be appropriately modified.

Figure 2 shows actual $f_{\mathrm{lab}}(\hat{\mathbf{k}}\cdot\hat{\mathbf{Z}})$ distributions computed for $\rho = 0.0$, 0.1, 0.2, 0.4, 0.8, and 1.6. The plots have been arbitrarily scaled to the peak heights of each plot, rather than to the total number of counts. The noise on these distributions results from the statistical nature of the Monte Carlo averaging procedure. Figure 3 gives computed $f(\hat{\mathbf{L}}\cdot\hat{\mathbf{Z}})$ distributions for these same values of ρ. In the RASKL limit, these are identical to

TABLE I. Monte Carlo values[a] of $\langle P_2(\hat{k}\cdot\hat{Z})\rangle$ and α_{RASKL} as a function of the universal beam-gas parameter ρ.[b]

ρ	$\langle P_2(\hat{k}\cdot\hat{Z})\rangle$	α_{RASKL}
0.0	1.000	−2.50
0.1	0.861	−2.19
0.2	0.772	−1.95
0.3	0.698	−1.75
0.4	0.636	−1.59
0.5	0.593	−1.51
0.6	0.541	−1.37
0.7	0.513	−1.30
0.8	0.476	−1.18
0.9	0.451	−1.16
1.0	0.423	−1.06
1.1	0.407	−1.02
1.2	0.388	−1.01
1.3	0.368	−0.94
1.4	0.352	−0.92
1.5	0.312	−0.81
1.6	0.308	−0.77
1.7	0.299	−0.75
1.8	0.294	−0.73
1.9	0.271	−0.71
2.0	0.270	−0.67

[a]Computed by averaging over 5000 events. One standard deviation corresponds to ~1.4%.

[b]Defined as $T_g M_b/T_b M_g$, where T and M are temperatures and masses and g and b refer to gas and beam species.

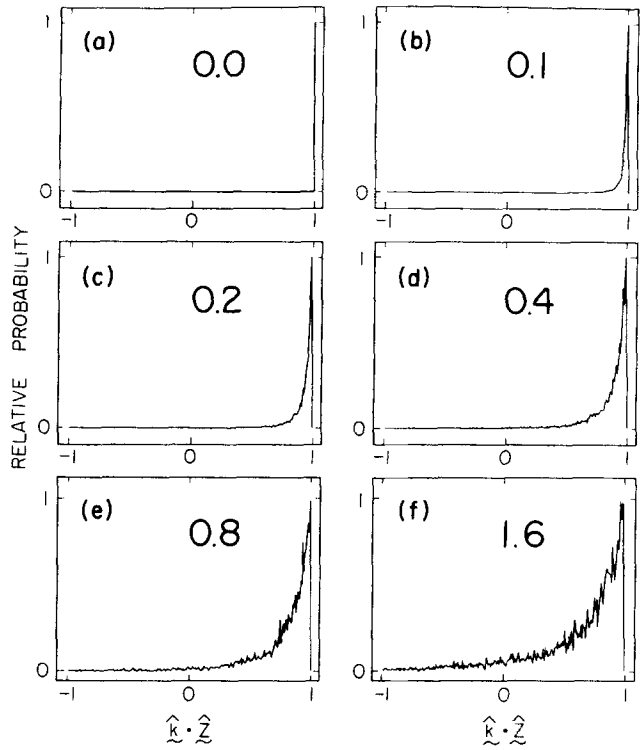

FIG. 2. The $f_{lab}(\hat{k}\cdot\hat{Z})$ distributions computed by the Monte Carlo method for a range of ρ values. The value of ρ is indicated in each case. The maximum peak height in each distribution is normalized to unity.

$f_{obs}(\hat{J}'\cdot\hat{Z})$ because under these conditions the product internal angular momentum $\mathbf{J}'$ equals the reagent orbital angular momentum $\mathbf{L}$ as discussed in Sec. II B.

It is necessary to distinguish between the distribution of relative velocity vectors *existing* in a beam–gas con-

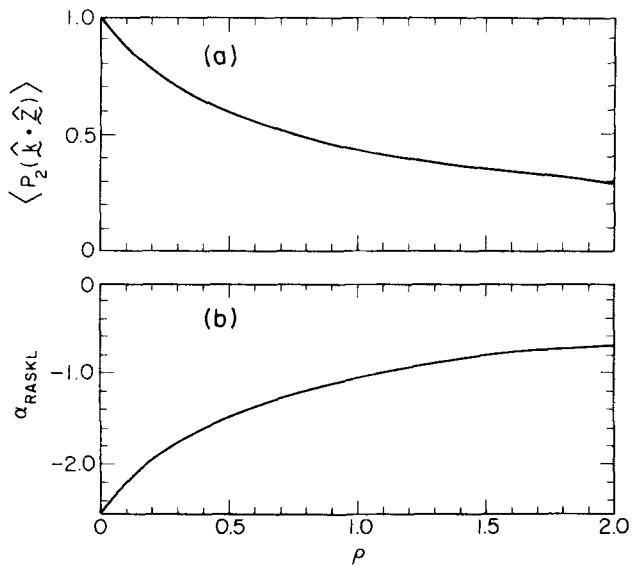

FIG. 1. Variation of (a) $\langle P_2(\hat{k}\cdot\hat{Z})\rangle$ and (b) α_{RASKL} with the universal beam–gas parameter ρ.

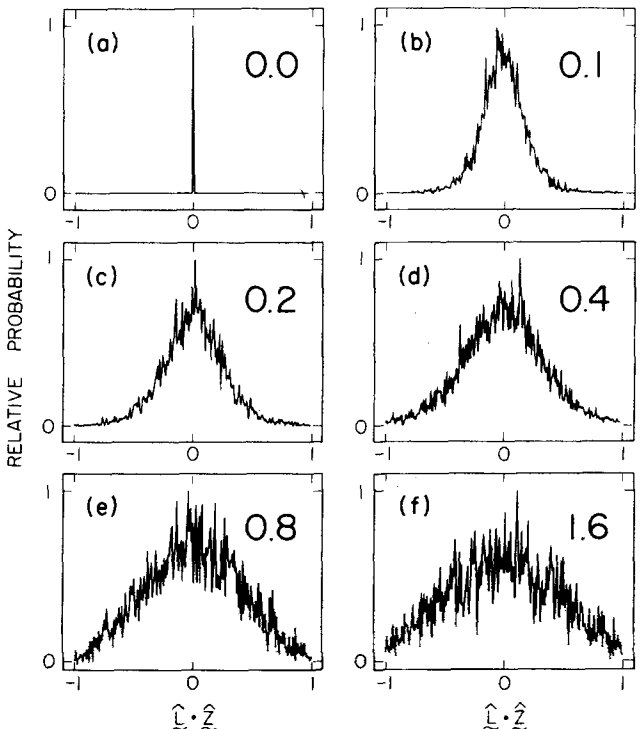

FIG. 3. The $f(\hat{L}\cdot\hat{Z})$ distributions computed by the Monte Carlo method for various ρ values. The value of ρ is indicated in each case. The maximum peak height in each distribution is normalized to unity. In the RASKL limit $f(\hat{L}\cdot\hat{Z}) = f_{obs}(\hat{J}'\cdot\hat{Z})$.

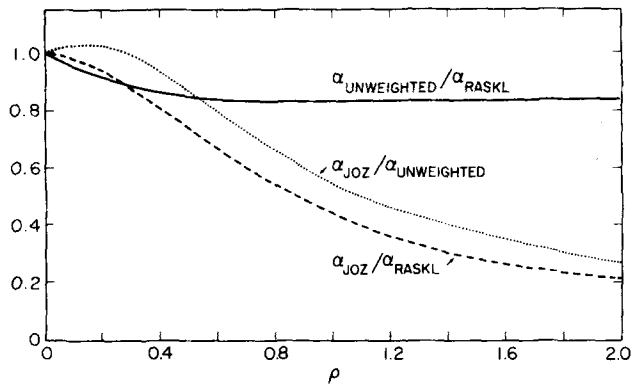

FIG. 4. Variation of alignment parameter ratios as a function of ρ.

figuration and the effective *reactive* distribution which is weighted for collision flux. The solid curve in Fig. 4 shows the ratio $\alpha_{UNWEIGHTED}/\alpha_{RASKL}$ as a function of ρ, where $\alpha_{UNWEIGHTED}$ is the value of the alignment parameter computed without this weighting. It is seen that this weighting grows in importance as ρ increases.

For completeness, we have added the ratios $\alpha_{JOZ}/\alpha_{RASKL}$ (dashed curve) and $\alpha_{JOZ}/\alpha_{UNWEIGHTED}$ (dotted curve) to Fig. 4. We see that Eq. (17) cannot reproduce our values of α_{RASKL}, which is not surprising considering the approximations made in its derivation. However, we note that $\alpha_{JOZ}/\alpha_{UNWEIGHTED} \simeq 1$ for $\rho \lesssim 0.4$, indicating that the omission of the weighting factors of Eq. (18) constituted the major error in this range.

III. MEASUREMENT OF CL POLARIZATION FROM THE REACTION $Ca(^1D) + HCl \rightarrow CaCl^*(B\,^2\Sigma^+) + H$

Brinkman *et al.*[32] have shown that the reaction of hydrogen chloride gas with calcium atoms in the metastable $4s3d\,^1D$ state produces visible chemiluminescence originating from the CaCl $A\,^2\Pi$ and $B\,^2\Sigma^+$ states and terminating on the $X\,^2\Sigma^+$ ground state. We choose to study the CL polarization of the reaction $Ca(^1D) + HCl \rightarrow CaCl(B\,^2\Sigma^+) + H$ because the mass combination exemplifies a kinematically constrained system and the CaCl $B\,^2\Sigma^+ - X\,^2\Sigma^+$ chemiluminescence is a parallel-type transition.

A. Experimental procedure

The beam–gas apparatus is similar to that described previously.[5,33] Depending on configuration it can take chemiluminescence spectra, measure the polarization of chemiluminescent features, and obtain the dependence of a chemiluminescent feature on beam velocity. Only the main points are summarized here.

The calcium sample is loaded into a graphite oven suspended inside a resistively heated graphite tube. Metastable calcium atoms are produced by an intense discharge which is struck between the oven orifice and the heating tube. Normally a dc discharge of 1.0 A is employed. In TOF experiments the discharge is pulsed on for 10 μs at a repetition rate of 2000 Hz.

The static HCl gas is at a pressure of $\sim 10^{-1}$ Pa (10^{-4} Torr). Its temperature can be varied by cooling a 10 cm diameter copper box that almost completely surrounds (~ 11 sr) the reaction zone.

The chemiluminescence spectrum is taken with a $\frac{3}{4}$ m monochromator using a 1200 groove/mm grating blazed at 600 nm. An 8 cm focal length lens collects ~ 0.1 sr of the chemiluminescence and focuses the reaction zone on the entrance slit of the monochromator. For polarization measurements, a polarization scrambler is placed before the entrance slit. It consists of two commercially available (Karl Lambrecht) birefringent wedges held with their faces parallel and their optic axes making an angle of 45°. With this device the response of the detection system is found to be independent of polarization of the incident light. Between the polarization scrambler and the lens is inserted a polarization analyzer, consisting of a sheet of polaroid.

TOF spectra were recorded using a boxcar signal averager (PAR model 162 with a model 165 plugin). A gate width of 10 μs is used in the "RUN" mode.

B. Experimental results

Figure 5 presents the $\Delta v = 0$ sequence portion of the CaCl B–X chemiluminescence spectrum. This was recorded with a resolution of 0.02 nm (FWHM) using a Ca oven temperature of 1200 K and an HCl gas temperature of 293 K. As is characteristic of the visible band systems of the alkaline earth monohalides, the $\Delta v = 0$ sequence has almost all the intensity. Band heads are formed in the P_1 and P_2 branches. Their vibrational numbering is based on the recent analysis of Berg *et al.*[34] The R branch lines contribute to the underlying background. The spectrum we have obtained is essentially identical to that observed by Brinkman *et al.*[32]

Having verified the identity of the emitter, subsequent experiments were carried out under the same conditions but with the monochromator set to a resolution of 0.1 nm (FWHM) and fixed on the peak found at 593.52 nm (marked by an arrow in Fig. 5). This feature has been assigned[34] to the overlap of the P_1 head of the (0, 0) band

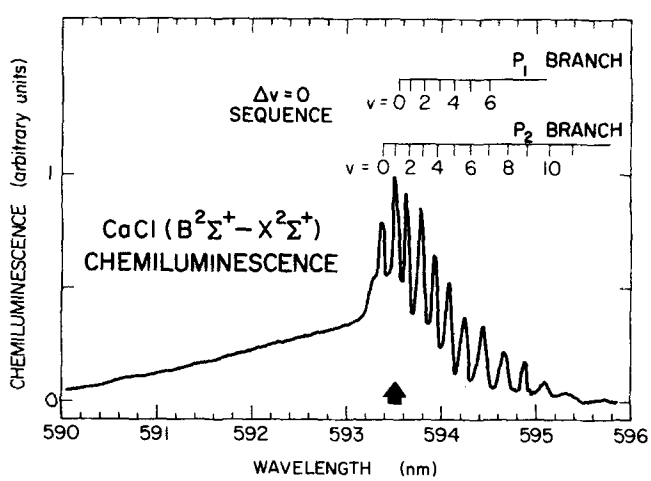

FIG. 5. Portion of the chemiluminescence spectrum resulting from the beam-gas reaction $Ca(^1D) + HCl$. The arrow marks the spectral region for which polarization and TOF measurements were made.

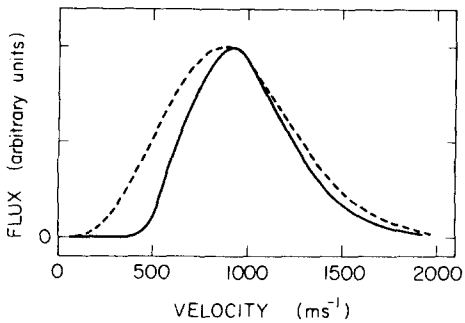

FIG. 6. Velocity distribution of those Ca (^1D) atoms which react with HCl to produce CaCl B–X chemiluminescence (solid curve). This distribution is derived from a TOF spectrum recorded following the pulsed production (10 μs duration) of a discharge at the oven orifice. The dashed curve shows the velocity distribution calculated for an effusive Ca beam at the oven temperature of 1200 K.

and the P_2 head of the (1, 1) band, corresponding to emission from $v'=0$ and 1. The CL polarization of this CaCl B–X feature was measured for two temperatures of the HCl gas. We find for $T_g=293\pm2$ K

$$P_{CL}=0.22\pm0.01 \tag{20}$$

and for $T_g=150\pm10$ K,

$$P_{CL}=0.25\pm0.01\ . \tag{21}$$

Similar values of P_{CL} are found throughout the $\Delta v=0$ sequence. The degree of polarization is positive and sizable, as anticipated for this kinematically constrained reaction system. Moreover, P_{CL} increases with decreasing gas temperature.

In order to check for the existence of a translational barrier in the reaction entrance channel, a TOF spectrum was also recorded. The data have been inverted to give the velocity distribution shown as a solid curve in Fig. 6. This velocity distribution applies to those beam species responsible for the observed chemiluminescence. For comparison a dashed curve has been added to Fig. 6 giving the velocity distribution calculated for an effusive beam, i.e., $f(v_b)=v_b^3\exp(-M_b v_b^2/2kT_b)$ for $M_b=40$ and $T_b=1200$ K. We conclude that no appreciable translational barrier is present. The slight narrowing of the actual beam profile is attributed largely to a departure from purely effusive behavior.

IV. DISCUSSION

The interpretation of vector correlations in beam–gas scattering experiments requires a knowledge of the distribution $f_{lab}(\hat{k}\cdot\hat{Z})$ of relative velocity directions $\hat{k}$ with respect to the beam direction $\hat{Z}$. We have shown that $f_{lab}(\hat{k}\cdot\hat{Z})$ can be calculated to any desired degree of accuracy by a Monte Carlo sampling procedure. Moreover, we have found that the second Legendre moment, $\langle P_2(\hat{k}\cdot\hat{Z})\rangle$, of this distribution can be expressed as a function of the single universal kinematic parameter $\rho=(M_b T_g)/(M_g T_b)$.

The values of $\langle P_2(\hat{k}\cdot\hat{Z})\rangle$ given in Table I and shown in Fig. 1 are a measure of the width of the angular spread in $f_{lab}(\hat{k}\cdot\hat{Z})$. It is apparent from these values and from the simulated distributions presented in Fig. 2 that $f_{lab}(\hat{k}\cdot\hat{Z})$ remains highly anisotropic over the range of ρ considered ($0\le\rho\le2$).

From the measured degree of chemiluminescence polarization, P_{CL}, one determines, using Eq. (6), the alignment parameter $\alpha=5\langle P_2(\hat{J}'\cdot\hat{Z})\rangle$ which is proportional to the second Legendre moment of the distribution $f_{obs}(\hat{J}'\cdot\hat{Z})$ of product angular momentum directions about the beam axis. Once $\langle P_2(\hat{k}\cdot\hat{Z})\rangle$ is known (from the above Monte Carlo calculations), then the dynamical quantity $\langle P_2(\hat{J}'\cdot\hat{k})\rangle$ of product angular momentum directions about the relative velocity vector, can be extracted by dividing $\langle P_2(\hat{J}'\cdot\hat{Z})\rangle$ by $\langle P_2(\hat{k}\cdot\hat{Z})\rangle$. Therefore one can picture $\langle P_2(\hat{k}\cdot\hat{Z})\rangle$ as an effective "resolution" with which $f_{c.m.}(\hat{J}'\cdot\hat{k})$ can be studied in a beam–gas chemiluminescent reaction. As ρ decreases $\langle P_2(\hat{k}\cdot\hat{Z})\rangle$ increases. Hence, the observed degree of CL polarization can be enhanced by merely reducing the value of ρ. This can be accomplished by raising the temperature of the beam or by lowering the temperature of the target gas. In practice the gas temperature is more easily varied. In any event, the observed degree of polarization is likely to be within a factor of two of its hypothetical value obtained in the absence of relative velocity vector averaging.

The dependence on ρ of the limiting degree of CL polarization P_{RASKL} for a beam-gas experiment is given in Fig. 7. This was calculated directly by the Monte Carlo procedure described in Sec. IIC, but is fully consistent with polarization values calculated from $\langle P_2(\hat{k}\cdot\hat{Z})\rangle$ using Eq. (16). This limiting polarization reaches its maximum possible value of one-third at $\rho=0$ and falls monotonically with increasing values of ρ. At $\rho=1$, P_{RASKL} has decreased by a factor of 2.0. In this case, $T_g/T_b=M_g/M_b$. In a typical beam–gas experiment $T_b\simeq4\,T_g$ so that $\rho=1$ requires $M_b\simeq4\,M_g$. For most chemiluminescent reactions studied to date, $M_b<4\,M_g$, i.e., in most cases of practical interest ρ is less then unity.

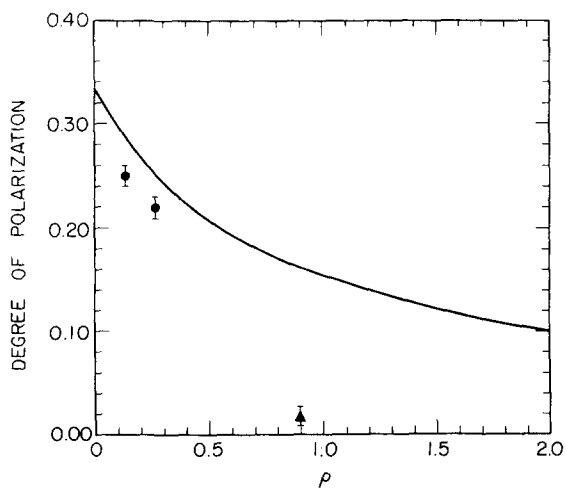

FIG. 7. Calculated limiting degree of beam–gas CL polarization (solid curve) as a function of ρ. The two circles represent the results of this study for the reaction Ca (^1D) + HCl; the triangle refers to the reaction Ba + NO_2 reported in Ref. 5.

TABLE II. Values of $\langle P_2(\hat{J}' \cdot \hat{k})\rangle$ for beam-gas chemiluminescent reactions.

Emitter	P_{CL}	ρ	$\langle P_2(\hat{J}' \cdot \hat{Z})\rangle$	$\langle P_2(\hat{k} \cdot \hat{Z})\rangle$	$\langle P_2(\hat{J}' \cdot \hat{k})\rangle$
CaCl(B)	0.22 ± 0.01	0.267 ± 0.005	-0.316 ± 0.014	0.72 ± 0.02	-0.44 ± 0.02
CaCl(B)	0.25 ± 0.01	0.137 ± 0.009	-0.364 ± 0.016	0.83 ± 0.03	-0.44 ± 0.03
BaO(A)	0.02 ± 0.005	0.78 ± 0.005	-0.027 ± 0.008	0.48 ± 0.01	-0.06 ± 0.02

Three experimental points have been added to Fig. 7. The two solid circles are the values of P_{CL} for the reaction $Ca(^1D) + HCl \rightarrow CaCl(B\,^2\Sigma^+) + H$ presented in Sec. III B. Values of ρ for these two points are calculated as 0.267 ($T_g = 293$ K, $T_b = 1200$ K) and 0.137 ($T_g = 150$ K, $T_b = 1200$ K). The solid triangle represents the value of $P_{CL} = 0.020 \pm 0.005$ for the reaction $Ba + NO_2 \rightarrow BaO(A\,^1\Sigma^+) + NO$, reported by Jonah *et al.*[5] From their experimental conditions ($T_g = 293$ K, $T_b = 1100$ K) we estimate $\rho = 0.78$. It is seen that the small polarization observed is *not* merely a consequence of relative velocity vector averaging; at $\rho = 0.78$, $P_{RASKL} = 0.16$. In sharp contrast, the CL polarizations for $CaCl(B\,^2\Sigma^+)$ reported here closely approach P_{RASKL}.

Table II lists the values of $\langle P_2(\hat{J}' \cdot \hat{k})\rangle$ determined from P_{CL} and ρ for each reaction. It is seen that the two different values of P_{CL} for the $Ca(^1D) + HCl$ reaction obtained at different gas temperatures yield the *same* value of $\langle P_2(\hat{J}' \cdot \hat{k})\rangle$ within the experimental uncertainty. As expected, the value of $\langle P_2(\hat{J}' \cdot \hat{k})\rangle$ for the kinematically unconstrained reaction $Ba + NO_2$ is much smaller, indicating a more nearly isotropic distribution of $\hat{J}'$ about $\hat{k}$. Nevertheless, a comparison with the product rotational alignment data reported to date (Table III) shows that this value of $\langle P_2(\hat{J}' \cdot \hat{k})\rangle$ is not unusual for such cases.

The value of $\langle P_2(\hat{J}' \cdot \hat{k})\rangle$ obtained for the $Ca(^1D) + HCl$ chemiluminescent reaction indicates a highly polarized distribution of product angular momentum directions in the center of mass frame. A value of -0.45 for $\langle P_2(\hat{J}' \cdot \hat{k})\rangle$ is equivalent to a value of 0.033 for $\langle |\hat{J}' \cdot \hat{k}|^2\rangle$, i.e., the average angle between $\mathbf{J}'$ and $\mathbf{k}$ is of the order of 80°. Thus $\mathbf{J}'$ is confined to a fairly narrow disk perpendicular to $\mathbf{k}$. Similar results have been obtained by Hsu *et al.*[12] for the reactions Cs + HI, Cs + HBr, and K + HBr (see Table III). The values of $\langle P_2(\hat{J}' \cdot \hat{k})\rangle$ obtained by the electric deflection method of Cs + HI and K + HBr agree with one another and with our value for $Ca(^1D) + HCl$ to within experimental errors. The result for Cs + HBr is only slightly smaller. This confirms the contention that kinematics dominate these $H' + HL \rightarrow H'H + L$ reaction systems.[4] Nevertheless, none of the results precisely attains the RASKL limit of $\langle P_2(\hat{J}' \cdot \hat{k})\rangle = -\frac{1}{2}$, in which $\mathbf{J}'$ is exactly perpendicular to $\mathbf{k}$. Clearly other factors can affect the product alignment.

How kinematically constrained is the $Ca(^1D) + HCl \rightarrow CaCl(B\,^2\Sigma^+) + H$ reaction system? In the RASKL limit both J and $\mathbf{L}'$ vanish, causing $\mathbf{L} = \mathbf{J}'$. We consider how large might be the deviations from $|\mathbf{L}| \gg |\mathbf{J}|$ and $|\mathbf{J}'| \gg |\mathbf{L}'|$. Taking a typical "harpoon" mechanism[4] impact parameter of 0.3 nm and a relative velocity of 10^5 cm/s, we find $|\mathbf{L}| \simeq 90\hbar$. This is indeed much larger than the average rotational angular momentum of the HCl gas, for which we estimate $|\mathbf{J}| \simeq 4\hbar$. For the product orbital angular momentum, kinematic relations require[12]

$$|\mathbf{L}'| = |\mathbf{J}'|[(M_H E_T')/(M_{Ca} E_R')]^{1/2} b'/r' , \qquad (22)$$

where M_H and M_{Ca} are the masses of the H and Ca atoms, E_T' and E_R' are the product translational and rotational energies, and b' and r' are the exit impact parameter and the $CaCl(B\,^2\Sigma^+)$ internuclear distance, respectively. Reasonable estimates of the above quantities suggests that $|\mathbf{J}'| \geq 5|\mathbf{L}'|$. It appears that the H atom *can* carry away significant orbital angular momentum in spite of its small mass. The same conclusion for the K + HBr system has been reached by Case and Herschbach,[15] and indeed had been anticipated by a theoretical calculation of Suplinskas and Ross.[36] Thus some deviation from the RASKL limit is reasonable for the $Ca(^1D) + HCl$ system. From conservation of angular momentum with $\mathbf{J} = 0$ it follows that $\mathbf{J}' = \mathbf{L} - \mathbf{L}'$. Hence, $\mathbf{J}'$ will not be exactly parallel to $\mathbf{L}$ but instead is distributed about it by forming the resultant of $\mathbf{L}$ with the randomly oriented $\mathbf{L}'$. Indeed, if $|\mathbf{J}'| \simeq 5|\mathbf{L}'|$ and these vectors are uncorrelated, this would quantitatively account for the observed deviation of $\langle P_2(\hat{J}' \cdot \hat{k})\rangle$ from the RASKL limit. Further discussion of the dynamical significance of $\langle P_2(\hat{J}' \cdot \hat{k})\rangle$ must await the outcome of experiments in which DCl replaces HCl and in which different product states are systematically examined.

TABLE III. Summary of product alignment data.

Method	Reaction	Collision energy (kJ mol^{-1})	$\langle P_2(\hat{J}' \cdot \hat{k})\rangle$
Electric deflection	Cs + HI	10	-0.44 ± 0.04[a]
	Cs + HBr	9	-0.38 ± 0.04[a]
	K + HBr	8	-0.42 ± 0.06[a]
	K + Br_2	Thermal beams ($\lesssim 10$)	-0.12[b]
	Cs + Br_2		-0.10[b]
	Cs + CF_3I (CsI)		-0.12[b]
	Cs + CH_3I		-0.12[b]
	Cs + CCl_4		-0.06[b]
	Cs + SF_4		-0.02[b]
	Cs + SF_6		-0.04[b]
Crossed beam chemiluminescence	Xe^m + Br_2	6	-0.14 ± 0.03[c]
	Xe^m + CCl_4		-0.01 ± 0.01[c]
	Xe^m + ICl (XeCl*)		-0.01 ± 0.02[c]
	Xe^m + CH_3I		-0.23 ± 0.03[c]
	Xe^m + CF_3I (XeI*)		-0.07 ± 0.07[c]
	Xe^m + BrCN (CN*)		0.00 ± 0.02[d]
Beam-gas chemiluminescence	Ca^m + HCl	7	-0.44 ± 0.02[e]
	Ba + NO_2	7	-0.05 ± 0.02[f]

[a]Reference 12.
[b]Reference 11.
[c]Reference 9.
[d]Reference 35.
[e]Present work.
[f]Reference 5.

ACKNOWLEDGMENTS

We are indebted to G. M. McClelland for valuable discussions. This work is supported by the National Science Foundation under NSF CHE 78-10019.

[1]M. R. Levy, Prog. React. Kinet. 10, 1 (1979).
[2]I. W. M. Smith, *Kinetics and Dynamics of Elementary Gas Reactions* (Butterworths, London, 1980).
[3]R. B. Bernstein, Adv. At. Mol. Phys. 15, 167 (1979).
[4]D. R. Herschbach, Discuss. Faraday Soc. 33, 283 (1962); Adv. Chem. Phys. 10, 319 (1966).
[5]C. D. Jonah, R. N. Zare, and Ch. Ottinger, J. Chem. Phys. 56, 263 (1972).
[6]C. T. Rettner and J. P. Simons, Chem. Phys. Lett. 59, 178 (1978).
[7]C. T. Rettner and J. P. Simons, Faraday Discuss. Chem. Soc. 67, 329 (1979).
[8]R. J. Hennessy and J. P. Simons, Chem. Phys. Lett. 75, 43 (1980).
[9]R. J. Hennessy, Y. Ono, and J. P. Simons, Mol. Phys. (in press); J. P. Simons (private communication).
[10]C. Maltz, N. D. Weinstein, and D. R. Herschbach, Mol. Phys. 24, 133 (1972).
[11]D. S. Y. Hsu and D. R. Herschbach, Faraday Discuss. Chem. Soc. 55, 116 (1973).
[12]D. S. Y. Hsu, N. D. Weinstein, and D. R. Herschbach, Mol. Phys. 29, 257 (1975).
[13]D. S. Y. Hsu, G. M. McClelland, and D. R. Herschbach, J. Chem. Phys. 61, 4927 (1974).
[14]D. S. Perry, A. Gupta, and R. N. Zare, in *Proceedings of the Industrial and Scientific Conference Management Inc.*, Chicago, 1981 (to be published).
[15]D. A. Case and D. R. Herschbach, Mol. Phys. 30, 1537 (1975); J. Chem. Phys. 64, 4212 (1976); 69, 150 (1978).
[16]D. A. Case, G. M. McClelland, and D. R. Herschbach, Mol. Phys. 35, 541 (1978).
[17]G. M. McClelland and D. R. Herschbach, J. Phys. Chem. 83, 1445 (1979); Faraday Discuss. Chem. Soc. 67, 360 (1979).
[18]N. H. Hijazi and J. C. Polanyi, J. Chem. Phys. 63, 2249 (1975); Chem. Phys. 11, 1 (1975).
[19]A. Kafri, Y. Shimoni, R. D. Levine, and S. Alexander, Chem. Phys. 13, 323 (1976).
[20]K. Schulten and R. G. Gordon, J. Chem. Phys. 64, 2918 (1976).
[21]M. H. Alexander, P. J. Dagdigian, and A. E. DePristo, J. Chem. Phys. 66, 59 (1977).
[22]M. P. Sinha, C. D. Caldwell, and R. N. Zare, J. Chem. Phys. 61, 491 (1974).
[23]A. J. McCaffery, S. R. Jeyes, and M. D. Rowe, Ber. Bunsenges. Phys. Chem. 81, 225 (1977).
[24]R. E. Drullinger and R. N. Zare, J. Chem. Phys. 51, 5532 (1969); J. Chem. Phys. 59, 4225 (1973).
[25]C. T. Rettner, L. Wöste, and R. N. Zare, Chem. Phys. (in press).
[26]M. Menzinger, Adv. Chem. Phys. 42, 1 (1980).
[27]P. Soleillet, Ann. Phys. (Paris) 12, 23 (1929); F. Perrin, J. Phys. Radium 7, 390 (1926); Ann. Phys. (Paris) 12, 169 (1929).
[28]G. Weber, Adv. Protein Chem. 8, 415 (1953).
[29]R. N. Porter and L. M. Raff, in *Modern Theoretical Chemistry* (Plenum, New York, 1976), Vol. 2, pp. 1–52.
[30]M. G. Prisant, W. M. Ollison, and R. J. Cross, Jr., J. Chem. Phys. 69, 4797 (1978).
[31]M. G. Prisant, Ph.D. thesis (in preparation).
[32]U. Brinkmann and H. Telle, Mol. Phys. 39, 361 (1980); Chem. Phys. Lett. 73, 530 (1980).
[33]T. Kiang, R. C. Estler, and R. N. Zare, J. Chem. Phys. 70, 5925 (1979).
[34]L. E. Berg, L. Klynning, and H. Martin, Phys. Scr. 22, 216 (1980).
[35]R. J. Hennessy, Y. O'Connor, and J. P. Simons, Chem. Phys. Lett. 75, 47 (1980).
[36]R. J. Suplinskas and J. Ross, J. Chem. Phys. 47, 321 (1967).